OPTIMAL PLACEMENT AND SIZING OF A UNIFIED POWER FLOW CONTROLLER IN A POWER SYSTEM NETWORK TO MINIMIZE POWER LOSS USING VOLTAGE SENSITIVITY INDEX AND BAT ALGORITHM

Musa, S.Y., Haruna, J., Ibrahim, V.M.* and Abdullahi, A.

Department of Electrical and Electronics Engineering, Modibbo Adama University, Yola, Nigeria

*Corresponding email: visaibrahim@gmail.com

ABSTRACT

Enhancing the power transfer capability of transmission lines in a power system network has become a critical concern, particularly as modern power systems grow in size, complexity, and energy demand. The introduction of Flexible Alternating Current Transmission System (FACTS) technology provides an alternative approach to improving power system performance. Among various FACTS devices, the Unified Power Flow Controller (UPFC) stands out as the most versatile due to its ability to regulate voltage magnitude, phase angle, and line impedance. To maximize the benefits of a FACTS device, determining its optimal location and size is essential. This study employs the Voltage Sensitivity Index (VSI) method to identify the best placement for the UPFC, while the Bat Algorithm (BA) optimization technique is used to determine its appropriate size. The proposed approach is tested on the IEEE 14-bus network, demonstrating a reduction in active and reactive power losses from 13,593 MW and 56,910 MVAr to 13,491 MW and 22.5715 MVAr, respectively. Additionally, the maximum bus voltage improves from 1.0466 pu to 1.0626 pu (a 1.53% increase). The obtained results are further compared with similar studies in the literature. Future studies should explore hybrid FACTS device, real time optimization algorithms and stability for larger grids, considering dynamic condition and renewable energy integration.

Keywords: Unified Power Flow Controller, Voltage Sensitivity Index, Bat Algorithm

1 INTRODUCTION

Electrical power supply serves as a fundamental pillar and a key driving force behind development and technological advancements in modern society. Due to increasing energy demands, existing power networks are continuously expanded and upgraded to meet growing requirements. However, several challenges hinder optimal power system performance, leading to an ongoing search for methods to enhance reliability, efficiency, quality, and stability. One widely adopted approach is the integration of Flexible Alternating Current Transmission Systems (FACTS) devices. As stated in [1], FACTS devices are power electronics-based solutions combined with static controllers to improve system controllability and maximize power transfer capacity. These controllers can operate based on both current-source or voltage-source principles and are classified into four categories: series-connected controllers, shunt-connected controllers, combined series-series controllers, and combined shunt-series controllers. Among the various FACTS devices, the Unified Power Flow Controller (UPFC) is the most flexible, as it can regulate key system parameters, including: Phase angle, Bus voltage, Transmission line reactance between two buses. The UPFC can adjust these parameters either independently or simultaneously [2]. Proper placement and parameter tuning of the UPFC in the network can significantly enhance overall performance. Several studies have primarily focused on identifying the optimal UPFC location [3, 4, 5]. This research, however, simultaneously addresses both the placement and sizing of the UPFC. The Voltage Sensitivity Index (VSI) is utilized for identifying the most suitable location, while the Bat Algorithm (BA) is employed for determining the optimal UPFC size.

2 METHODOLOGY

This study follows a structured approach: Development and implementation of steady state power flow analysis based on Newton-Raphson for the study system in other to determine pre compensation (base case) bus voltages, power available on the buses and the power loss in each branch of the network. Computation of voltage sensitivity indices (VSIs) for all the load buses of the study system to determine the weakest bus which is the optimal location for UPFC placement in the network. Determination of optimal size of the UPFC using bat algorithm. Validate the effectiveness of the work on the IEEE 14 bus test network.

2.1 Power Flow Analysis

A power system operates under various voltage and power conditions at its buses, ensuring compliance with standard requirements. Power Flow Analysis (PFA), extensively discussed in power system literature, is a widely applied method for determining feasible operating states by leveraging known bus parameters. The primary objective of power flow analysis is to compute system bus voltages (both magnitude and angle), assess power adjustments at generation buses, and determine power flow across transmission lines [6]. This study focuses on steady-state analysis, where system parameters remain unchanged over time. Once the system's steady-state conditions are established, it becomes possible to estimate the required generation capacity to meet demand and evaluate power losses within the network. Power flow analysis primarily involves solving the intricate and nonlinear power balance equations presented in equations (1) and (2).

$$P_i = \sum_{i=1}^{N} |V_i||V_j||Y_{ij}| \cos(\delta_i - \delta_j - \theta_{ij}), j = 1, \ldots, N \quad (1)$$

$$Q_i = \sum_{i=1}^{N} |V_i||V_j||Y_{ij}| \sin(\delta_i - \delta_j - \theta_{ij}), j = 1, \ldots, N \quad (2)$$

Where: i = 1…, N, N is the number of load buses; Pi = active power generated or injected on bus i; Qi = reactive power generated or injected on bus i; $|Vi|$ = voltage module of bus i; δi = voltage angle of bus i, yij = element of the nodal admittance matrix $Ybus$. The nodal admittance matrix is developed thus; if i = j, yij is the sum of the admittances that come out of the bus i; and if $i \neq j$, yij is the admittance between the buses i and j, multiplied by -1. The power system buses are categorized into three depending on which variables are known and which variables are to be obtained through the power flow analysis. The bus types are, Load bus (PQ Bus): Pi & Qi are specified and $|Vi|$ and δi are obtained through the PFA; Generator bus (PV Bus): Pi & $|Vi|$ are specified and Qi and δi are obtained through the PFA; Slack bus (Vδ Bus): $|Vi|$ and δi are specified and Pi and Qi are obtained through the PFA. Since power balance equations are nonlinear, they are solved using numerical computational techniques such as the Newton-Raphson method. These methods involve initializing estimated values for bus voltage magnitudes and angles—typically 1.0 pu and 0 rad, respectively—and then refining these values through successive iterations to obtain better approximations. The iterative process continues until the desired level of accuracy is achieved.

2.2 Computation of Voltage Sensitivity Indices

A reliable way to determine the areas in a power system where instability is most likely to occur is by identifying the weakest bus. The weakest bus is characterized by insufficient reactive power support, making it the most vulnerable to voltage collapse. Several methods for identifying weak buses have been proposed in the literature [7] and applied in studies such as [8]. Most of these methods rely on voltage sensitivity analysis. Voltage sensitivity indices are widely used as indicators of voltage stability, with several types developed for this purpose. One such index that directly relates bus voltage to reactive power is the Reactive Power Voltage Sensitivity Index (RPVS). This index measures the variation in the voltage magnitude of bus i due to a unit reactive power injection at bus j [9]. The calculation of RPVS begins with the linearized form of the nonlinear power balance equations, as expressed in equation (3) [10].

$$\begin{bmatrix} \Delta P \\ \Delta Q \end{bmatrix} = \begin{bmatrix} J_1 & J_2 \\ J_3 & J_4 \end{bmatrix} \begin{bmatrix} \Delta \quad Q \\ \Delta \ |V| \end{bmatrix} \tag{3}$$

Where, matrix J is the Jacobean matrix, Pi and Qi are as in equations (1) and (2), ΔP and ΔQ are vectors of real and reactive bus power changes, while $\Delta\delta$ and ΔV are vectors of changes in bus voltage angles and voltage magnitudes respectively. From equation (3).

$$\Delta Q = \left(-J_3 \frac{J_2}{J_1} + J_4\right) \Delta |V| \tag{4}$$

Reactive power is primarily influenced by variations in voltage magnitudes and is less sensitive to changes in phase angles. Conversely, real power is highly sensitive to phase angle variations but minimally affected by voltage magnitude changes. Therefore, setting $\mathbf{J_2}$ and $\mathbf{J_3}$ in equation (4) to zero is a reasonable approximation, leading to the simplified form presented in equation (5).

$$\frac{\Delta |V|}{\Delta Q} = J_{4ij}^{-1} \tag{5}$$

The RPVSI are computed as in equation (6).

$$RPVS_i = diag\{J_{4ij}^{-1}\} \tag{6}$$

Bus with the smallest RPVS is the weakest in the system and most suitable bus for locating UPFC.

2.3 Bat Algorithm

The Bat Algorithm (BA) is a bio-inspired optimization technique introduced by Xin-She Yang in 2010. It has proven to be an effective and efficient optimization method [12]. Meta-heuristic algorithms like Particle Swarm Optimization (PSO) and Simulated Annealing (SA) are widely used for solving complex optimization problems. However, BA is considered a more powerful approach as it integrates key advantages of several popular heuristic algorithms [13]. It is particularly useful for addressing nonlinear and global optimization problems, offering simplicity, flexibility, and stability. BA is modeled after the echolocation ability of bats, which emit short, high-frequency sound pulses and listen for echoes that bounce back after hitting an object. By analyzing these echoes, bats can estimate distances, differentiate between obstacles and prey, and navigate efficiently—even in complete darkness. In the Bat Algorithm, frequency tuning is utilized, where each bat is represented with a velocity and a position in a *d*-dimensional solution space at iteration *t*. The bat's position corresponds to a solution vector for the given optimization problem. Among the *n* bats in the population, the best solution $x*$ found so far is retained throughout the iterative search process. Based on the echolocation principles of bats, the Bat Algorithm is formulated using the following three idealized rules:

2.3.1 Echolocation Ability

All bats use echolocation to measure distances and can somehow distinguish between prey (food) and background obstacles.

2.3.2 Random Flight Behavior

Bats move randomly with velocity (v_x), at position (x_i), with a frequency (f) or wavelength (λ), and a loudness (A_0) while searching for prey. They can dynamically adjust the wavelength (or frequency) of their emitted pulses and modify the pulse emission rate $r \in [0,1]$ based on their proximity to the target.

2.3.3 Loudness Variation

While loudness can change in various ways, it is assumed to decrease from an initial high value (A_0) to a minimal constant value (*Amin*). During the application of the Bat Algorithm, the positions (x_i) and velocities (v_i) in a *d*-dimensional search space are continuously updated. The new solutions (x_i□) and velocities (v□) at iteration *t* are determined using predefined update equations as;

$$f_i = f_{min} + (f_{max} - f_{min})\beta \tag{7}$$

$$V_i^t = V_i^{t-1} + \left(x_i^{t-1} - x^*\right) f_i \tag{8}$$

$$x_i^t = x_i^{t-1} + V_i^t \quad (9)$$

Where $\beta \in [0, 1]$ is a random vector drawn from a uniform distribution. x^* is the current global best location (solution) which is located after comparing all the solutions. Once a solution is selected among the current best solutions, a new solution for each bat is generated locally using random walk. Once a solution is selected among the current best solutions, a new solution for each bat is generated locally using random walk.

$$x_{new} = x_{old} + \epsilon A^t \quad (10)$$

$\epsilon \in [-1, 1]$ is a random number, while $A^t = < A_i^t >$ is the average loudness of all the bats at this step. In addition, the loudness A_i and pulse emission rates r_i can be varied during the iterations using the following equations.

$$A_i^{t+1} = \alpha A_i^t \quad (11)$$

And

$$r_i^{t+1} = r_i^0 [1 - \exp(-\gamma t) \quad (12)$$

Where $0 < \alpha < 1$ and $\gamma > 0$ are constants. For any $0 < \alpha < 1$ and $y > 0$, while the initial emission rate $r^0 \in [0, 1]$. The bat algorithm is summarized in the flow chart of Figure 1 [14].

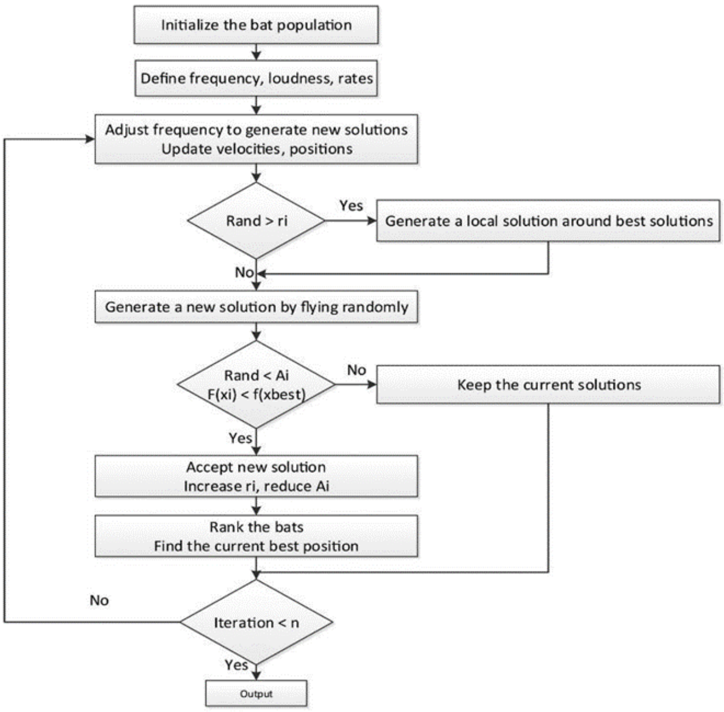

Figure 1. The bat algorithm flowchart [14]

2.4 Objective Function

The objective of this study is to reduce real power losses, thereby maximizing power transfer capability. Mathematically, the objective function is expressed as [11]:

$$f = \min(P_{loss}) \quad (13)$$

$$P_{loss} = V_j \sum_{j=1}^{Nb} G_{ij} [V_i^2 + V_j^2 - 2V_i V_j \cos(\delta_i - \delta_j) \quad (14)$$

Where Gij is the conductance of line ij, V_i and V_j are the magnitudes of sending end and receiving end voltages of the line. δ_i and δ_j are the phase angles of the end voltages. Ntl is the number of transmission lines. The equality constraints:

$$P_{Gi} - P_{Di} - V_j \sum_{j=1}^{Nb} V_j \left(G_{ij} \cos(\delta_i - \delta_j) + B_{ij} \sin(\delta_i - \delta_j)\right) = 0 \quad (15)$$

$$Q_{Gi} - Q_{Ci} - Q_{Di} - V_i \sum_{j=1}^{Nb} V_j \left(G_{ij}\sin(\delta_i - \delta_j) + B_{ij}\cos(\delta_i - \delta_j)\right) = 0 \quad (16)$$

P_{Gi} is the real power generation at bus i, P_{Di} is the power demand at bus i, Nb is the number of PQ nodes in the system. Q_{Gi} is the reactive power generation at bus i, Q_{Di} is the reactive power demand at bus i, Q_{Ci} is the reactive power from compensation nodes. The inequality constraints are: Voltage limits for generator buses:

$$V_{Gi}^{min} \leq V_{Gi} \leq V_{Gi}^{max} \quad (17)$$

Where V_{Gi}^{min} is the minimum voltage at the generator bus, VGi is the actual voltage at the generator bus and VGi^{max} is the maximum voltage of the generator bus. Real power generation limits:

$$P_{Gi}^{min} \leq P_{Gi} \leq P_{Gi}^{max} \quad (18)$$

Where P_{Gi}^{min} represents the minimum real power at the generator bus, P_{Gi} denotes the actual real power at the generator bus, and P_{Gi}^{max} is the maximum real power at the generator bus. Reactive power generation limits:

$$Q_{Gi}^{min} \leq Q_{Gi} \leq Q_{Gi}^{max} \quad (19)$$

Where Q_{Gi}^{min} is the minimum reactive power at the generator bus, Q_{Gi} represents the actual reactive power at the generator bus, and Q_{Gi}^{max} is the maximum reactive power at the generator bus. UPFC limits.

$$V_{vi}^{min} \leq V_{vi} \leq V_{vi}^{max} \quad (20)$$

Where V_{vr}^{min} is the minimum shunt converter voltage magnitude (p.u), Vvr is the actual shunt converter voltage (p.u) and V^{max} is the maximum shunt converter voltage magnitude (p,u).

$$V_{ci}^{min} \leq V_{ci} \leq V_{ci}^{max} \quad (21)$$

Where V_{cr}^{min} is the series converter voltage magnitude (p.u), V_{cr} is the actual series converter voltage magnitude (p.u) and V_{cr}^{max} is the maximum series converter voltage magnitude (p.u). The input parameters for the bat algorithm are given in table 1.

Table 1. Input parameter of table 1

S/N	Parameters Quantity
1	Number of iterations 50
2	Number of population 20
3	Pulse rate 0.9
4	Loudness 0.9

2.5 Study System and Data Presentation

The research is based on the IEEE 14-bus system, which consists of 5 generator buses, 9 load buses, and 20 transmission lines. The system's one-line diagram is illustrated in Figure. 2, while the bus and branch data are provided in Tables 2 and 3, respectively.

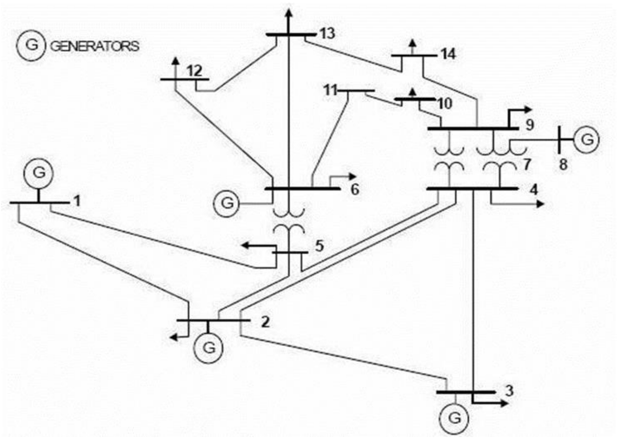

Figure 2. One- line diagram of IEEE 14 bus system [15]

Table 2. Bus Data of IEEE 14 Bus Network [15]

Bus No.	Bus Type	Volt Mag. (pu)	Angle Degree	PG MW	QG MVA R	PL MW	QL MVA R
1	Slack	1.06	0	232.4	-16.9	0	0
2	PV	1.045	-4.98	40	42.4	21.7	12.7
3	PV	1.01	-12.72	0	23.4	94.2	19
4	PQ	1.019	-10.33	0	0	47.8	-3.9
5	PQ	1.02	-8.78	0	0	7.6	1.6
6	PV	1.07	-14.22	0	12.2	11.2	7.5
7	PQ	1.062	-13.37	0	0	0	0
8	PV	1.09	-13.36	0	17.4	0	0
9	PQ	1.056	-14.94	0	0	29.5	16.6
10	PQ	1.051	-15.1	0	0	9	5.8
11	PQ	1.057	-14.79	0	0	3.5	1.8
12	PQ	1.055	-15.07	0	0	6.1	1.6
13	PQ	1.05	-15.16	0	0	13.5	5.8
14	PQ	1.036	-16.04	0	0	14.9	5

Table 3. Line Data for IEEE 14 Bus System [15]

Line No.	From Bus	To Bus	Resistance (p.u)	Reactance (p.u)	Line Charging Susceptance (p.u)	Tap Ratio
1	1	2	0.01938	0.05917	0.0528	1
2	1	5	0.05403	0.22304	0.0492	1
3	2	3	0.04699	0.19797	0.0438	1
4	2	4	0.05811	0.17632	0.0374	1
5	2	5	0.05695	0.17388	0.034	1
6	3	4	0.06701	0.17103	0.0346	1
7	4	5	0.01335	0.04211	0.0128	1
8	4	7	0	0.20912	0	0.978
9	4	9	0	0.55618	0	0.969
10	5	6	0	0.25202	0	0.932
11	6	11	0.09498	0.1989	0	1
12	6	12	0.12291	0.25581	0	1
13	6	13	0.06615	0.13027	0	1
14	7	8	0	0.17615	0	1
15	7	9	0	0.11001	0	1
16	9	10	0.03181	0.0845	0	1
17	9	14	0.12711	0.27038	0	1
18	10	11	0.08205	0.19207	0	1
19	12	13	0.022092	0.19988	0	1
20	13	14	0.17093	0.34802	0	1

3 RESULTS AND DISCUSSION

The outcomes of the research, following modeling and simulation, include:

3.1 Optimal Location of UPFC

The calculated reactive power voltage stability indices for the studied system are presented in Table 4. In Table 4, the bus with the lowest RPVS is identified as the weakest in the system, making it the most suitable location for placing the UPFC. Consequently, bus 14 is determined to be the optimal placement.

Table 4. Voltage Sensitivity Indices for Study System

Load Bus Number	Voltage Stability Index
4	0.0827
5	0.0516
7	0.1116
9	0.0632
10	0.3421
11	0.0451
12	0.2723
13	0.0448
14	0.0260

3.2 Optimal Size of UPFC

The optimal UPFC size was determined using the bat algorithm optimization technique. For the IEEE 14-bus network, the calculated optimal size of the UPFC is 18.1737 MVAr.

3.3 Validation of the Proposed Technique

Power flow analysis was conducted using the Newton-Raphson method both before and after UPFC compensation. The percentage increase in bus voltages, compared to their pre-compensation values, is presented in Table 5.

Table 5. Bus Voltage Improvement

Bus Number	Bus Voltage (pu)		Enhancement (%)
	Before UPFC	After UPFC	
1	1.0600	1.0600	0.00
2	1.0450	1.0450	0.00
3	1.0100	1.0100	0.00
4	1.0132	1.0147	0.15
5	1.0166	1.0175	0.09
6	1.0700	1.0700	0.00
7	1.0457	1.0517	0.57
8	1.0800	1.0900	0.93
9	1.0305	1.0364	0.57
10	1.0299	1.0348	0.48
11	1.0461	1.0486	0.24
12	1.0533	1.0619	0.82
13	1.0466	1.0626	1.53
14	1.0193	1.0297	1.02

Likewise, the real and reactive power loss reductions for each branch of the network were computed both before and after compensation. The percentage reduction in power loss, relative to the pre-compensation values, is presented in Table 6.

Table 6. Reduction in Line Real and Reactive Power Loss

Line Number	From Bus	To Bus	Real Power Loss			Reactive Power Loss		
			Before UPFC	After UPFC	Reduction (%)	Before UPFC	After UPFC	Reduction (%)
1	1	2	4.3086	4.3041	0.10	13.1547	13.1410	0.10
2	1	5	2.7726	2.7695	0.11	11.4455	11.4326	0.11
3	2	3	2.3352	2.3294	0.25	9.8298	9.8140	0.16
4	2	4	1.6700	1.6703	-0.02	5.0670	5.0682	-0.02
5	2	5	0.9200	0.9148	0.57	2.8089	2.7931	0.56
6	3	4	0.3911	0.3846	1.66	0.9983	0.9817	1.66
7	4	5	0.4791	0.4884	-1.94	1.5113	1.5406	-1.94
8	4	7	0	0	0	1.9317	2.1045	-8.95
9	4	9	0	0	0	1.2920	1.3363	-3.43
10	5	6	0	0	0	5.7736	5.6347	2.41
11	6	11	0.1227	0.1027	16.30	0.2568	0.2151	16.24
12	6	12	0.0806	0.0607	24.69	0.1678	0.1264	24.67
13	6	13	0.2518	0.2060	18.19	0.4960	0.4058	18.19
14	7	8	0	0	0	0.6679	0.8322	-24.60
15	7	9	0	0	0	0.9573	0.9665	-0.96
16	9	10	0.0060	0.0062	-3.33	0.0160	0.0165	-3.13
17	9	14	0.0894	0.0955	-6.82	0.1902	0.2032	-6.83
18	10	11	0.0514	0.0387	24.71	0.1203	0.0905	24.77
19	12	13	0.0110	0.0105	4.55	0.0100	0.0095	5.00
20	13	14	0.1054	0.1328	-26.00	0.2146	0.2703	-25.96

3.4 Comparison of Proposed Technique with Similar Work in Literature

The results indicate that voltage improvements were achieved on ten out of the fourteen buses after compensation, with a maximum increase of 1.53%. Likewise, a reduction in transmission losses was observed across most branches in the network. Therefore, results of this study affirm that the integration of VSI and BA for UPFC deployment is not only feasible but also competitive and, in some aspects, superior results compared to other approaches in existing literature especially in reactive power loss reduction and simplicity of the method [7, 10, 15]. The methodology offers strong loss mitigation, improved voltage stability, and computational efficiency, also its performance validates the effectiveness of combining analytical and metaheuristic techniques, offering a valuable contribution to ongoing UPFC research and application [8]. As power systems grow more complex, such hybrid techniques may play a pivotal role in practical FACTS device deployment strategies.

Table 7. Comparison of Proposed Work with Similar Work

Bus No.	Proposed			Aman and Jitendra [16]		
	Bus Voltage without UPFC	Bus Voltage with UPFC	% increase	Bus Voltage without UPFC	Bus Voltage With UPFC	% increase
1	1.0600	1.0600	0.00	1.060	1.0600	0.00
2	1.0450	1.0450	0.00	1.186	1.0450	-11.89
3	1.0100	1.0100	0.00	1.030	1.0100	-1.94
4	1.0132	1.0147	0.15	0.989	0.99795	0.90
5	1.0166	1.0175	0.09	0.918	1.0034	9.30
6	1.0700	1.0700	0.00	1.090	1.0700	-1.83
7	1.0457	1.0517	0.57	0.969	1.0349	6.80
8	1.0800	1.0900	0.93	1.110	1.0900	-1.80
9	1.0305	1.0364	0.57	0.989	1.0115	2.28
10	1.0299	1.0348	0.48	0.969	1.0109	4.32
11	1.0461	1.0486	0.24	0.967	1.0349	7.02
12	1.0533	1.0619	0.82	0.969	1.0461	7.96
13	1.0466	1.0626	1.53	0.987	1.0363	4.99
14	1.0193	1.0297	1.02	0.969	0.9968	2.87

4 CONCLUSIONS

This study calculates reactive power voltage sensitivity (RPVS) indices for the IEEE 14-bus system to identify the weakest bus, determining the most suitable location for UPFC placement. The analysis reveals that bus 14 is the weakest and, therefore, the optimal placement site. The Bat algorithm is utilized to determine the ideal UPFC compensator size, which is found to be 18.1737 MVAr. Simulations on the compensated system indicate an increase in bus voltages across most buses, though the improvements are relatively minor (with a maximum increase of 1.53% at bus 13). This is attributed to the system's inherent compensators at buses 3, 6, and 8. Overall, voltage profiles improved on ten out of fourteen buses, with the highest voltage enhancement from 1.0466 p.u to 1.0626 p.u (1.53%). Additionally, the greatest reduction in real and reactive power losses occurs on line 18, decreasing from 0.0514 p.u to 0.0387 p.u (24.71%) and from 0.1203 p.u to 0.0905 p.u (24.77%), respectively. Compared to similar approaches, this method proves more effective in enhancing voltage across a greater number of buses.

REFERENCES

1. Hingorani, G. and Gyugi, L. (1999). Understanding FACTS: Concepts and Technology of Flexible AC Transmission Systems. *IEEE Press*, pp. 1-37.

2. Nabavi-Niaki, A. and Iravani, MR. "Steady State and Dynamic Models of Unified Power Flow Controller (UPFC) for Power System Studies. *IEEE Transactions on Power Systems*, vol. 11, no. 4, pp. 1937-1943.

3. Arabkhaburi, D., Kazemi, A., Yari, M. and Aghaei, J. (2006). Optimal placement of UPFC in power systems using genetic algorithm. *IEEE International Conference on Industrial Technology*, pp. 1694-1699.

4. Fadi, M.A., Shameem, A., Sa'ad, M., Hazlie, M. and Hassan, M.A. (2015). Optimal placement of unified power flow controller to improve dynamic voltage stability using power system variable based voltage stability indices. *Journal of Testing and Evaluation*, vol. 10, no. 4, pp. 1-32.

5. Ghahremani, E. and Kamwa, I. (2013). Optimal Placement of Multiple-Type FACTS Devices to Maximize Power System Loadability Using a Generic Graphical User Interface. *IEEE Transactions on Power Systems*, vol. 28, no. 2, pp. 764-778.

6. Pruthviraja, L., Pradeepkumar, F.H., Ashok, M. and Mahesh Kumar, B.T. (2016). Load Flow Computation and Power Loss Reduction Using New Particle Swarm Optimization Technique. *International Journal of Scientific Development and Research*, vol. 1, no. 6, pp. 114-117.

7. Jitendra Singh Bhadoriya and Chandra Kumar Daheriya, (2014). An Analysis of Different Methodology for Evaluating Voltage Sensitivity. *International Journal of Advanced Research in Electrical, Electronics and Instrumentation Engineering*, vol. 3, no. 9, pp. 12239-12246.

8. Sharma, P.R., Ahuja, R.K., Vashisth, S. and Hudda, (2014). Computation of sensitive node for for IEEE-14 bus system subjected to load variation. *International Journal of Innovative Research in Electrical, Electronics, Instrumentation and Control Engineering*, vol. 2, no. 6, pp. 1603-1608.

9. Rodr´ıguez Monta˜n´es M., Riquelme, S.J. and Romero, R.E. (2005). **V**oltage Sensitivity Based Technique for Optimal Placement of Switched Capacitors *15th PSCC, Liege*, 22-26 August 2005 Session 16, pp. 4-6.

10. Pradyumna Roy, P., Bera, S.H. and Das, P.K. (2013). Reactive Power Sensitivity Index based Voltage Stability Analysis to a Real System (400KV System of WBSEB). *International Journal of Electronics & Communication Technology*, vol. 4, no. 1, pp. 1-7.

11. Cui, X., Gao, J., Feng, Y., Zou, C. and Liu, H. (2018). Multi-objective reactive power optimization based on improved particle swarm algorithm. *IOP Conference Series: Earth and Environmental Science, vol. 108*, no. 5, pp. 52-81.

12. Yang, X.S. and He, X. (2013). Bat Algorithm: Literature review and applications. *International Journal of Bio-Inspired Computation*, vol. 5, no. 3, pp. 141-149.

13. Yang, X.S. (2010). A New Metaheuristic Bat-Inspired Algorithm, in: Nature Inspired Cooperative Strategies for Optimization (NISCO 2010*)* (Eds. J. R. Gonzalez et. al.), Studies in Computational Intelligence, Springer Berlin, 284, Springer, pp. 65-74,

14. Shaoqiang, Y., Yang, Y., Mengjie, Z., Enze, W. and Lan, W. (2017). The economic benefit of liner ships with lower speed. *Advances in Mechanical Engineering*, vol. 9, no. 11, pp. 1-11.

15. University of Washington (2019). *Bus and line data of IEEE 14 bus system*. Retrieved from http://www.ee.washington.edu/research/pstca/pf14/pg_tca14bus.htm.

16. Aman, S. and Jitendra, S.B. (2017). Optimal Placement of Unified Power Flow Controller (UPFC) in IEEE 14 Bus System Using Genetic Algorithm (GA). *International Journal of Advances in Engineering and Scientific Research*, vol. 4, no. 2, pp. 15-30.